IEEE Access
Multidisciplinary | Rapid Review | Open Access Journal

Received February 19, 2020, accepted March 3, 2020, date of publication March 16, 2020, date of current version March 26, 2020.

Digital Object Identifier 10.1109/ACCESS.2020.2981137

Interference Mitigation Using Angular Diversity Receiver With Efficient Channel Estimation in MIMO VLC

MONA HOSNEY[1], HOSSAM A. I. SELMY[2], (Member, IEEE), ANAND SRIVASTAVA[3], (Member, IEEE), AND KHALED M. F. ELSAYED[4], (Senior Member, IEEE)

[1]National Telecommunication Institute, Cairo 11768, Egypt
[2]National Institute of Laser Enhanced Science (NILES), Cairo University, Giza 12613, Egypt
[3]Department of Electronics and Communications Engineering, IIIT-Delhi, New Delhi 110020, India
[4]Department of Electronics and Communications Engineering, Faculty of Engineering, Cairo University, Giza 12613, Egypt

Corresponding author: Mona Hosney (monyhosney@gmail.com)

ABSTRACT Visible Light Communication (VLC) is a promising solution to meet the ever increasing demand for indoor data connectivity with high bit rates. VLC uses the license-free bands and provides high-speed connections unlike RF wireless communication. However; indoor VLC suffers from performance degradation due to either co-channel interference (CCI) or inter-symbol interference (ISI). In this paper, an interference management scheme is proposed for VLC Multi-Input Multi-Output (MIMO) based systems. The scheme reduces the number of interfered signals by using a constrained field-of-view angular diversity receiver CFOV-ADR and then uses least-square (LS) channel estimation with maximum-likelihood (ML) equalizer to resolve the interfered signals. The proposed interference mitigation scheme using constrained-FOV-ADR with channel estimation IM-CFOV-CE enables frequency reuse of one. The bit-error-rate (BER) is calculated at various room positions with different receiver's heights and rotation angles. The performance evaluation results reveal that the proposed system can achieve a higher number of downlink channels and superior BER performance than that of without CCI management. Also, the proposed scheme has been compared with Time Division Multiple Access (TDMA) technique, and achieves enhanced performance at all positions and orientations of the ADR.

INDEX TERMS Angular diversity receiver (ADR), co-channel interference (CCI), interference mitigation, visible light communication (VLC).

I. INTRODUCTION

Communication revolution era with the explosive growth of broadband applications, Internet services, and the rapid increase of consumer demands for seamless mobile data connectivity, given that the majority of wireless data traffic is generated indoors, service providers are constantly looking for innovative solutions to provide robust indoor wireless coverage [1]. Visible light communication VLC, in the 380-780 nm wavelength using light-emitting diodes, has recently emerged as a promising solution to support and complement indoor RF communication systems, due to its capability to overcome the currently witnessed scarcity of the radio spectrum resources. VLC has many advantages over traditional RF communications. It is license-free with huge optical bandwidth, uses existing lighting infrastructure, has no electromagnetic interference (EMI) and has no interference from adjacent rooms [2]. On the other side, VLC suffers from many challenges like short coverage, field of view (FOV) alignment, up-link realizations, and dimming. Also, non-line-of-sight (NLOS) propagation which comes from multi-path reflections, can result in severe Inter-Symbol Interference (ISI), especially for signals with high data rates. Additionally, LEDs have limited transmission bandwidth about (30-50 MHz) and it is vital to reuse the optical frequency by neighbor LEDs to achieve higher capacities and data rates. This, in turn, results in Co-Channel Interference (CCI) between neighbors transmitters.

In VLC system, MIMO techniques can be used to overcome CCI problems. Practically, this can be realized by

The associate editor coordinating the review of this manuscript and approving it for publication was Parul Garg.

using the existing multiple illumination LEDs. However; the de-correlation of highly correlated MIMO-VLC channel matrix becomes the bottleneck [3], [4]. Recently, many schemes have been proposed for reducing channel correlation using different receivers. In [5]–[7], imaging and non-imaging receivers were used to reduce the channel correlation. Imaging receiver gives better performance than that of non-imaging one but at much higher complexity and extra optics. In [8], Angle-aided Mirror Diversity (AMDR) uses mirror placement and variation of the rotation angle of the photo-detector (PD) to reduce the channel correlation. ADR which contains multiple PDs distributed with different inclination angles to limit the range of captured rays was addressed in [9]–[14]. ADR is used to reduce channel correlation in MIMO systems, improve the coverage of optical wireless systems, increase signal-to-interference-ratio (SINR) and system throughput. Also, the FOV of the ADR can be adjusted to eliminate the CCI and reduce ISI by receiving a maximum of one LOS signal on each PD [15]. Clearly, ADR has a compact receiver size and it does not require hardware adjustment to enable receiver's mobility in contrast to other designs.

In downlink VLC system, MIMO techniques can implement parallel data transmission or spatial multiplexing to achieve lower channels correlation. A precoded MIMO is designed to decode independent streams that are transmitted simultaneously from different transmitters [16]. Although this technique achieves high spectral efficiency, it has high implementation complexity especially when a large number of LEDs are installed. In [4], [10], [11], [17] a comparison between Repetition Coding (RC), Spatial Modulation (SM), Spatial Multiplexing (SMP) was done. In RC, all transmitters simultaneously emit the same signal. In SM, only one transmitter is active for any symbol duration as a transmitter is only activated when the random spatial symbol to be transmitted matches the transmitter index. In SMP, independent data streams are sent simultaneously from all transmitters using the same optical frequency band. Clearly, SM gives better spectral efficiency than that of RC and it is more robust to high channel correlation compared to SMP. Obviously, SMP gives the maximum spectral efficiency but it requires perfect channel estimation to overcome the problem of CCI. However, the optical MIMO channel matrix was assumed to be perfectly known in most of the carried studies [4], [9]–[11], [14], [16], [17].

In this paper, CCI is mitigated in SMP based MIMO-VLC downlink channels by proposing efficient channel estimation scheme. The scheme relies on limiting the number of interfered LOS signals by implementing an upper bound on FOV of ADR's PDs. Also, the scheme exploits the reception of well known periodical pilot signals to achieve accurate estimation. Generally, two techniques are commonly used for channel estimation which are Least Square Error (LS) and Minimum-Mean-Square-Error (MMSE). In this paper, the LS is used as MMSE is more complex and it requires noise distribution to be known at the receiver [15], [18].

After estimating MIMO channel gains, an equalizer is used to decode the received signal. A comparison between Zero-Forcing (ZF), Zero-Forcing with Successive Interference Cancellation (ZF-SIC), and MMSE-SIC equalizers were done in [19]. In [20], ZF is compared with Maximum-Likelihood equalizer (ML). ML is the optimum detection method compared to ZF which amplifies the system noise. However, ML complexity grows exponentially with the order of modulation. In this paper, LS and ML schemes are used for channel estimation and signal detection, respectively.

Based on the above discussion, we outline the contributions of this paper are as follows:

- Increasing the overall capacity of the downlink VLC network by reallocating the same optical spectrum among neighboring transmitters (SMP MIMO with a frequency reuse factor of one) in contrast to the existing MIMO and multiplexing techniques.
- Constraining FOV of an ADR to manage CCI and reduce the correlation between MIMO channels. The FOV value is calculated under the condition that ADR receives a limited number of LOS signals at all positions and orientations.
- Proposing efficient and real-time channel estimation and decoding schemes with ultimately low computational complexities.
- The proposed interference mitigation scheme can function with any arbitrary layout of LED transmitters in contrast to most of the existing MIMO schemes that operate with predefined distributions.
- The proposed scheme considers the effect of non-synchronized transmitters, i.e. the transmitting signals from different LEDs are assumed to have random circuit and switching delays.
- Guaranteeing user connectivity, and maximizing the number of downlink channels received by each user at all positions and orientations. This enables full user mobility and facilities handover between different LEDs.

This paper is organized as follows, Section II describes the ADR channel in the VLC model. Section III describes the proposed CCI management scheme. Section IV presents the performance evaluation results. Finally, section V is for the conclusion.

The notation $(.)^T$, $\circledast$, and $\|.\|$ denote transpose, convolution, and the norm, respectively.

II. VLC SYSTEM MODEL

Intensity modulation and direct detection are the simplest and most commonly used modulation and demodulation technique used in VLC system. As shown in Fig. 1, a stream of binary data is modulated with On-Off-Keying in the electrical domain, then it is converted to an optical signal using LED. The optical signal propagates through the channel and is received by a photo-detector (PD). The PD converts optical signal to an appropriate electric current. The generated current is amplified and equalized, then demodulated to recover the transmitted signal. In VLC system, many LED bulbs are

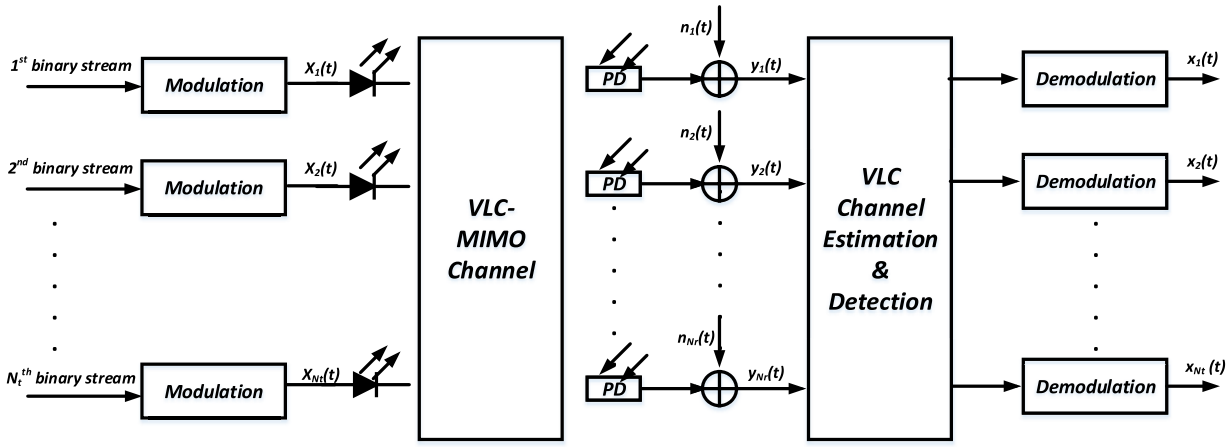

FIGURE 1. Illustration of the proposed VLC system.

installed in the room to produce sufficient illumination levels. Practically, a LED is modeled by a generalized Lambertian radiant intensity [21]:

$$R(\phi) = \frac{m+1}{2\pi} P_s \cos^m(\phi), \tag{1}$$

where ϕ is the angle of emission relative to the optical axis of the LED; m is the order of Lambertian emission given by $m = \frac{-\ln 2}{\ln(\cos(\Phi_{1/2}))}$ and $\Phi_{1/2}$ is semi half-angle (at half power).

A. MIMO VLC CHANNEL MODEL

The proposed optical MIMO system has N_t LEDs and ADR with N_r PDs, as shown in Fig. 2. The transmitted data are carried out through two types of VLC links. One is Line-of-sight (LOS) from point-to-point, and the other is Non-line-of-sight (NLOS) due to reflections [21], [22]. In most recent papers, the LOS link is only considered since it is usually much stronger than the NLOS link [4], [9], [14], [16]. However, the NLOS propagation is considered in evaluating the performance of the proposed scheme.

For a VLC MIMO system, the LOS channel response from the transmitted LED $j \in \{1, 2, \ldots, N_t\}$ to the PD $i \in \{1, 2, \ldots, N_r\}$ can be modeled by [21], [22]:

$$h_{ij}^{los}(t) = \begin{cases} \frac{(m+1)A_d}{2\Pi d_{ij}^2} \cos^m(\Phi_{ij}) \cos(\Theta_{ij}) & \\ \times \delta(t - \frac{d_{ij}}{c}), & \Theta_{ij} \le \psi \\ 0, & \Theta_{ij} > \psi \end{cases} \tag{2}$$

where A_d is the photo-detector active area, Φ_{ij} is the angle of irradiance at LED transmitter j with respect to PD i, Θ_{ij} is the incident angle at PD i with respect to LED transmitter j, d_{ij} is the distance from the LED j to the PD i, ψ is the photo-detector FOV, and c is the speed of light in free space as indicated in Fig. 3a.

On the other hand, the NLOS channel model caused by light reflections is calculated by dividing the room's walls into small reflecting elements K with reflection coefficient ρ and area ΔA, as shown in Fig. 3b. Each element k is treated as a small LED transmitter that emits the light to the PD i in Lambertian pattern of an attenuated version of the received signals. Without loss of generality, only the first order reflection is considered in the calculations as the

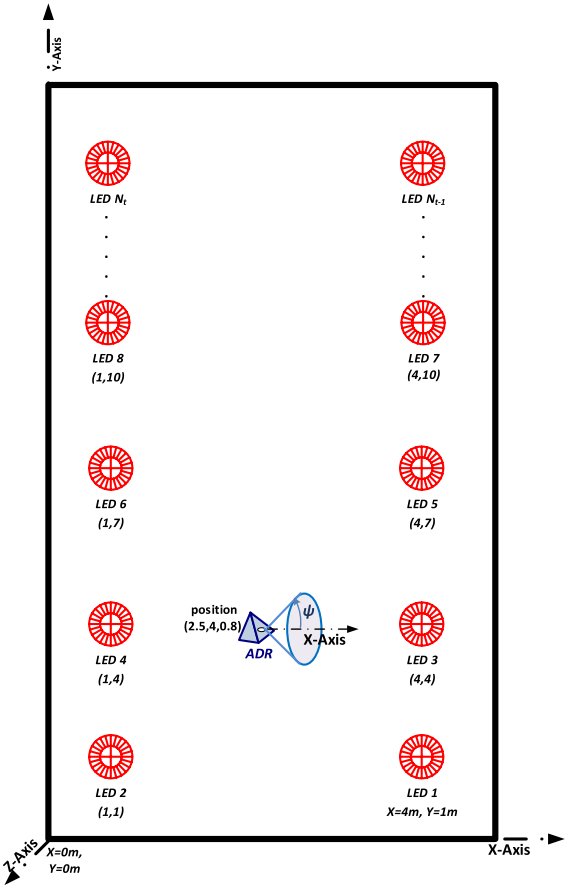

FIGURE 2. MIMO VLC system.

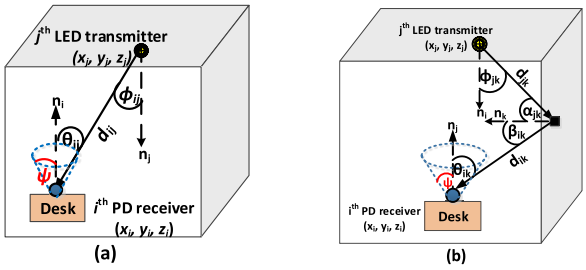

FIGURE 3. Downlink VLC channel Model (a) LOS (b) NLOS.

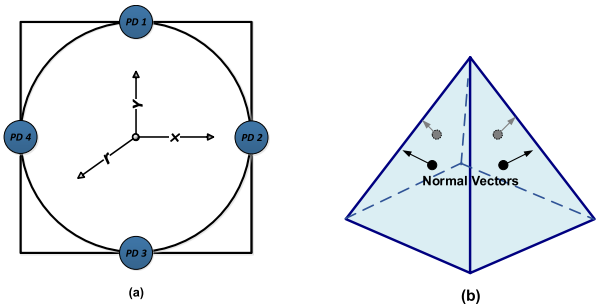

FIGURE 4. (a) The top view of a ADR receiver for $N_r = 4$ at $\gamma_R = 0$. (b) The proposed receiver with 4 PDs and their normal vectors.

higher order reflections have much less power and can be neglected [21], [22]. The NLOS channel response from the transmitted LED j to the PD i can be modeled by [21], [22]:

$$h_{ij}^{Nlos}(t) = \begin{cases} \sum_{k=1}^{K} \frac{(m+1)A_d \Delta A \rho_k}{2\pi^2 d_{jk}^2 d_{ik}^2} \cos^m(\Phi_{jk}) \cos(\alpha_{jk}) \\ \times \cos(\beta_{ik}) \cos(\Theta_{ik}) \delta(t - \frac{d_{jk}+d_{ik}}{c}), \quad \Theta_{ik} \le \psi \\ 0, \quad \Theta_{ik} > \psi \end{cases} \tag{3}$$

where d_{jk} is the distance from the LED $j \in \{1, 2, \ldots, N_t\}$ to the center of reflection point $k \in \{1, 2, \ldots, K\}$, K is the total number of the wall elements, Φ_{jk} is the angle of irradiance at LED transmitter j with respect to reflecting point k, α_{jk} is the angle of incidence at reflecting element k with respect to LED transmitter j, d_{ik} is the distance from the center of reflection point k to the PD $i \in \{1, 2, \ldots, N_r\}$, β_{ik} is the irradiance angle at reflecting element k with respect to PD i, and Θ_{ik} is the incidence angle at PD i relative to reflecting element k. Finally, the generated photo-currents $y(t) = [y_1(t); y_2(t); \ldots; y_{N_r}(t)]$ for all PDs are given by [23]:

$$y(t) = RH(t) \circledast x(t) + n(t), \tag{4}$$

where R is the PD responsivity, $x(t) = [x_1(t); x_2(t); \ldots; x_{N_t}(t)]$ is the optical intensity modulated signal vector of all transmitters, $n(t) = [n_1(t); n_2(t); \ldots; n_{N_r}(t)]$ is Additive White Gaussian Noise (AWGN) added to the system with zero mean, and variance $\sigma_n^2 = \sigma_{th}^2 + \sigma_{shot}^2$, where σ_{th}^2 is thermal noise that results from receiver electronics, and σ_{shot}^2 is the shot noise that results from received ambient light [24], $H(t)$ is $N_r \times N_t$ matrix summarized by the impulse responses between all transmitters and PDs as:-

$$H(t) = \begin{bmatrix} h_{11}(t) & \ldots & h_{1N_t}(t) \\ \vdots & \ddots & \vdots \\ h_{N_r1}(t) & \ldots & h_{N_rN_t}(t) \end{bmatrix}. \tag{5}$$

where $h_{ij}(t)$ is the sum of LOS and NLOS channel gain between the j^{th} LED and i^{th} PD and is defined by:

$$h_{ij}(t) = h_{ij}^{los}(t) + h_{ij}^{Nlos}(t). \tag{6}$$

The output current at each PD i is calculated as:

$$\begin{aligned} y_i(t) &= R \sum_{j=1}^{N_t} h_{ij}(t) \circledast x_j(t) + n(t). \\ &= R \sum_{j=1}^{N_t} \{h_{ij}^{los}(t) + h_{ij}^{Nlos}(t)\} \circledast x_j(t) + n(t). \end{aligned} \tag{7}$$

B. ADR RECEIVER DESCRIPTION

In the considered VLC MIMO system, ADR with N_r PDs is used to construct the multiple outputs. The PDs are arranged uniformly on a circle with radius r on a small horizontal plane as shown in Fig. 4a to form an ADR. The main idea of the ADR design is to vary the normal vector of each PD such that the incident angles from the same LED are different. Obviously, there are many ways for arranging the PDs, which change the orientation of normal vectors. In this paper, the pyramid shape is considered for the proposed scheme. Also, as the ADR has a small size, the distance between the same LED and all PDs are assumed nearly the same. The ADR parameters can be summarized by [9], [25], [26]:

- For $1 \le i \le N_r$, the coordinates of PD i in the pyramid receiver (PR) are given by:

$$\begin{aligned} &(x_{PD}^i, y_{PD}^i, z_{PD}^i) \\ &= (x_r + r\cos\frac{2(i-1)\pi}{N_r}, y_r + r\sin\frac{2(i-1)\pi}{N_r}, z_r), \end{aligned} \tag{8}$$

  where (x_r, y_r, z_r) are the coordinates of the center of the PD body and they can be varied by $x_r \in [0, L_x]$, $y_r \in [0, L_y]$ and $z_r \in [0, L_z]$, where L_x, L_y and L_z are the length, width, and height of the room, respectively.
- The elevation angle, the angle from positive z-axis due to the vertical rotation, can be varied in the range $[0, \pi]$. Hence, the total resulting elevation angle of i^{th} PD δ_{PD}^i can be expressed as $\delta_{PD}^i = \delta_r + \delta_{tilt} \in [0, \pi]$, $i \in \{1, \ldots, N_r\}$ where δ_{tilt} is the tilt angle of N_r PDs.
- The Azimuth angle of PD i (the angle from the positive x-axis) is given by:

$$\gamma_{PD}^i = \frac{2(i-1)\pi}{N_r} + \gamma_R, \tag{9}$$

where, $\gamma_R \in [0, 2\pi]$ is the whole receiver horizontal orientations angle.

- The coordinates (x, y, z) of normal vector $\hat{n}_i$ associated with PD i can be calculated from the elevation and azimuth angle by [25]:

$$\hat{n}_i = \begin{bmatrix} \cos(\gamma_r^i)\sin(\delta_{PD}^i) \\ \sin(\gamma_r^i)\sin(\delta_{PD}^i) \\ \cos(\delta_{PD}^i) \end{bmatrix}. \quad (10)$$

The LOS and NLOS channel impulse response for the link between the LED j and the PD i can be calculated from (2) (3), respectively.

III. PROPOSED INTERFERENCE MITIGATION SCHEME BASED ON CONSTRAINED FOV WITH CHANNEL ESTIMATION

The objective here is to increase the VLC's downlink capacity by allocating the whole optical bandwidth to each transmitted LED, i.e. frequency reuse of one. However, in this approach, the transmitted signals from neighbor LEDs can result in severe CCI unless an efficient interference management scheme is adapted to recover the interfered signals.

Towards that the number of interfered LOS signals on the ADR is limited by reducing the FOV angle of the PDs at all positions and orientations. The proposed ADR is called a Constrained-FOV-ADR (CFOV-ADR) in which the FOV angle is optimized so that the ADR receives a maximum of N_r LOS signals from N_t LEDs at all positions and orientations. After limiting the number of interfered signals, an efficient channel estimation scheme is proposed based on pilot transmission and least square (LS) method optimization. Finally, Maximum-Likelihood (ML) detection is used to resolve the interfered data streams while reducing their bit-error-rates (BER). Hence, the proposed scheme is called interference mitigation based on constrained FOV with channel estimation IM-CFOV-CE scheme.

A. CONSTRAINED FOV-ADR

The PDs of constrained FOV-ADR have FOV angle that limits the number of interfered LOS signals and reduces the effect of ISI. However, to realize channel estimation, the number of receiving antennas must be larger than or equal to the number of transmitters so that the channel gain matrix is not rank deficient [27]. Therefore, to estimate the LOS channel gains between different N_t transmitting LEDs and N_r PDs, the number of LOS signal received on these PDs N_{los} has to be less than or equal to N_r, i.e. $N_r \geq N_{los}$. In other words, the CCI could be efficiently mitigated and resolved if the number of LOS interfered signals is less than or equal to the number of used PDs. To satisfy this important condition, the FOV angle ψ (constant for all PDs) is optimized to get the optimum field of view angle ψ_{opt} (maximum value) which limits the number of received LOS signals N_{los} at all positions and orientations to N_r signals. However, to ensure proper operation of CFOV-ADR, we assume that the receiver has a gravity adjustment mechanism, so it would always point upwards with $\delta_r = 0^o$. Generally, for VLC system consists of N_t LEDs and N_r PDs, the $N_r \times N_t$ LOS channel gain matrix between all LED transmitters and PDs is given by:

$$H_{los} = \begin{bmatrix} h_{11}^{los}(x_r, y_r, z_r, \gamma_r, \psi) & \dots & h_{1N_t}^{los}(x_r, y_r, z_r, \gamma_r, \psi) \\ \vdots & \ddots & \vdots \\ h_{N_r1}^{los}(x_r, y_r, z_r, \gamma_r, \psi) & \dots & h_{N_rN_t}^{los}(x_r, y_r, z_r, \gamma_r, \psi) \end{bmatrix}, \quad (11)$$

where $h_{ij}^{los}(x_r, y_r, z_r, \gamma_r, \psi)$ represents the LOS channel gain between the LED j and PD i at the ADR position, orientation and FOV angle. Furthermore, an indicator I_j is used to show that the ADR receives a LOS signal from LED number j at each position, orientation and FOV angle $(x_r, y_r, z_r, \gamma_r, \psi)$ as:

$$I_j(x_r, y_r, z_r, \gamma_r, \psi) = \begin{cases} 0, & \text{if } \sum_{i=1}^{N_r} h_{ij}^{los}(x_r, y_r, z_r, \gamma_r, \psi) = 0, \\ & \forall j \in \{1, 2, \dots, N_t\}. \\ 1, & \text{if } \sum_{i=1}^{N_r} h_{ij}^{los}(x_r, y_r, z_r, \gamma_r, \psi) \geq 0, \\ & \forall j \in \{1, 2, \dots, N_t\}. \end{cases} \quad (12)$$

Then, the number of LOS received signals N_{los} at each $(x_r, y_r, z_r, \gamma_r, \psi)$ is calculated as:

$$\begin{aligned} & N_{los}(x_r, y_r, z_r, \gamma_r, \psi) \\ & \quad \triangleq \sum_{j=1}^{N_t} I_j(x_r, y_r, z_r, \gamma_r, \psi), \\ & \text{s.t. } 0 \leq x_r \leq L_x, 0 \leq y_r \leq L_y, \quad 0 \leq z_r \leq L_z, \\ & \quad \gamma_r \in [0, 2\pi], \quad \psi \in [0, \frac{\pi}{2}]. \end{aligned} \quad (13)$$

Although decreasing the value of the FOV angle reduces the number of received LOS signals, it decreases their received powers and associated signal to noise ratios. Therefore, there is an optimal FOV angle ψ_{opt} which is the maximum FOV angle that limits the number of received LOS signals at all positions and orientations to N_r as:

$$\begin{aligned} \psi_{opt} = & \max_{x_r, y_r, z_r, \gamma_r} \psi, \\ & \text{s.t. } N_{los}(x_r, y_r, z_r, \gamma_r, \psi) \leq N_r. \end{aligned} \quad (14)$$

Clearly, if ψ is higher than ψ_{opt}, the ADR will receive from more than N_r transmitters at some positions or orientations. In this situation, the channel gain matrix becomes rank deficient and its estimation will not be accurate. Consequently, the interfered signals will not be efficiently resolved, and CCI could not be mitigated. On the other side, if ψ is less than ψ_{opt}, the LOS channel gains will be decreased resulting in lower signal-to-noise (SNR) ratios and system capacity.

Practically, it is not possible to obtain one optimal FOV value that operates efficiently for several LED layouts.

This is because using fixed FOV angle value, the layouts with optimal FOV greater than this value will face a reduction in received SNRs and even having cut-off LOS links at some positions and orientations, while layouts with optimal FOV greater than this value will suffer from unresolved CCI. Thus, no sign for statistical averaging could be realized for all LED layouts. Therefore, we proposed to use an ADR with an adaptive FOV angle for its PDs. In this way, the designed ADR with an adaptive FOV angle is flexible and the performance could be enhanced for any LED layout.

Generally, the value of ψ_{opt} depends on both the room geometry and the LEDs layout. Obviously, it is hard to obtain a closed form for ψ_{opt} and instead, an exhaustive search is used to compute it offline. The computed value is stored at the transmitter's controller which sends it periodically in the downlink transmission. The existing ADRs use the received value to adjust the FOV angle of their PDs. This could be practically realized using mechanical iris, liquid crystal micro-lenses, micro-electronic-mechanical systems (MEMS) and adaptive optics [28]–[32].

After determination of ψ_{opt} which limits the number of received LOS signals to a maximum of N_r signals at all positions and orientations, the room with N_t LEDs is divided into L disjoint regions. In each region, the ADR receives LOS signals from certain N_r LEDs only. For each region l, $l \in \{1, 2, \ldots, L\}$, the associated N_r LED indices are summarized in set A_l. Hence, all possible (non-repeated) combinations of received LED indices at all positions and orientations can be represented as a set of sets:

$$A = \{A_1, A_2, \ldots, A_l, \ldots, A_L\},$$
$$\text{s.t. } A_l \notin (A - A_l), \quad l \in \{1, 2, \ldots, L\}. \tag{15}$$

where L is the total number of possible non-repeated sets of received indices at all positions and orientations and it depends on room geometry and LED distributions. Clearly, at each position and orientation $(x_r, y_r, z_r, \gamma_r)$, the indices of received N_r LOS signals are summarized in set $A(x_r, y_r, z_r, \gamma_r) \in A$.

Example 1: From the simulation of VLC downlink channel with 4 PDs ADR, indicated in Fig. 2, the optimal FOV angle $\psi_{opt} = 31^\circ$ and the channel gain matrix at position $(2.5, 4, 0.8)$ with $\gamma_r = 0^\circ$ is given by:

$$H_{los} = 1.0e-05 * \begin{bmatrix} 0 & 0 & 0 & 0 & 0 & 0 & 0 & 0 \\ 0 & 0 & 0.4584 & 0 & 0 & 0 & 0 & 0 \\ 0 & 0 & 0 & 0 & 0 & 0 & 0 & 0 \\ 0 & 0 & 0 & 0.4584 & 0 & 0 & 0 & 0 \end{bmatrix}. \tag{16}$$

The ADR receives a LOS signal from LEDs 3 and 4 only because the other LEDs are out of the ADR's FOV. It is worth noting that LEDs 1, 2, 5 and 6 have equal distances and directions to the ADR and ψ_{opt} is selected to prevent the reception of these interfered signals. Also, at any position and orientation, the ADR can receive LOS signals from one of the following sets: $A_1 = (1, 2, 3, 4), A_2 = (2, 3, 4, 6)$ and $A_3 = (1, 3, 4, 5)$.

Example 2: From the simulation of VLC downlink channel, indicated in Fig. 2, The channel gain matrix for an ADR at position $(2.5, 2.5, 0.8)$ with $\gamma_r = 0^\circ$ and $\psi_{opt} = 31^\circ$ is given by:

$$H_{los} = 1.0e-05 * \begin{bmatrix} 0 & 0 & 0.2311 & 0.2292 & 0 & 0 & 0 & 0 \\ 0.2292 & 0 & 0.2311 & 0 & 0 & 0 & 0 & 0 \\ 0.2292 & 0.2231 & 0 & 0 & 0 & 0 & 0 & 0 \\ 0 & 0.2231 & 0 & 0.2292 & 0 & 0 & 0 & 0 \end{bmatrix}. \tag{17}$$

The indices set $A(2.5, 2.5, 0.8, 0^\circ) = A_1 = \{1, 2, 3, 4\}$ and the ADR receives four LOS signals from LEDs 1, 2, 3 and 4. The other LEDs 5, 6, 7 and 8 are out of ADR's FOV. Furthermore, each PD receives two interfered LOS signals with nearly the same channel gain values. To resolve the CCI and recover the interfered signals, channel estimation is required to predict the channel gains associated with these signals. However, before estimating the channel gains, the indices of N_r transmitters (out of N_t) associated with the received LOS signals have to be determined first. Moreover, the estimated channel gains are used by a maximum-likelihood equalizer to decode the interfered signals. Obviously, increasing the number of decoded LOS signals for some users can easily duplicate their downlink channel capacities.

B. TRANSMITTERS DETERMINATION

Using proposed CFOV-ADR, the number of interfered LOS signals on ADR is less than or equal to the number of PDs N_r. Clearly, to resolve these interfered signals, their channel gains have to be first predicted using estimation techniques. In most studies, the optical MIMO VLC channel matrix was assumed to be perfectly known [4], [9]–[11], [14], [16], [17]. However; perfect channel estimation is not always available due to the nature of optical wireless channels. In the proposed IM-CFOV-CE scheme, before making the channel estimation, the N_r transmitters associated with received N_r signals have to be first determined. In other words, at each position and orientation $(x_r, y_r, z_r, \gamma_r)$, the indices of received N_r LOS signals summarized in $A(x_r, y_r, z_r, \gamma_r)$ are first determined. Toward determination of associated N_r transmitters at each position and orientation of the ADR, different well known N_t pilot signals are periodically transmitted from different transmitters. In other words, each LED transmits periodical unique well-known pilot pattern. Clearly, training sequence (TS) based channel estimation is one of the best known techniques. It works by sending different pilot signals from different LEDs [15]. OOK pilot training modulated sequence vector $P^j(t) = [P_1(t), P_2(t), \ldots, P_q(t)]$, is periodically sent from LED $j \in \{1, 2, \ldots, N_t\}$ with length of q bits. These pilots are used to cope with any channel variations or user movement. Generally, VLC channel faces slow

variations. Therefore, resending period must not be short and small transmission overhead is generated. Also, small circuit switching delays are assumed between the transmitted pilot signals. The received signal for these pilots at PD i is given as:

$$S^i(t) = \sum_{j=1}^{j=N_t} h_{ij}(t) \circledast P^j(t), \forall i \in \{1, 2, \ldots, N_r\}, \quad (18)$$

where, $h_{ij}(t)$ is the channel gain between LED j and PD i. The received signals from N_r PDs can be represented by the $N_r \times q$ matrix $S = [S^1(t), S^2(t), \ldots, S^{N_r}(t)]^T$. At the receiver side, perfect clock recovery is assumed to estimate delays between the received patterns. For each set of LEDs indices $A_l, l \in \{1, 2, \ldots, L\}$, an estimated pilot pattern $N_r \times q$ matrix $\hat{S}^l$ is generated with the estimated delays as:

$$\hat{S}^l = [P^b(t)], b \in \{A_l\}, \quad l \in \{1, 2, \ldots, L\}. \quad (19)$$

In order to determine the LEDs indices from which the ADR receives LOS signals, correlation is used. Specifically, for each set of possible LEDs indices A_l, the correlation coefficient C_l is measured between the generated pilot patterns matrix $\hat{S}^l$ and the received signal matrix S. The correlation coefficient measures the strength and direction of a linear relationship between two matrices [33]. The value of C_l lies between $[1, -1]$ and is calculated as [33], [34]:

$$C_l = \frac{\sum_{m=1}^{N_r} \sum_{n=1}^{q} (S_{mn} - \mu_s)(\hat{S}^l_{mn} - \mu_{\hat{S}^l})}{\sqrt{(\sum_{m=1}^{N_r} \sum_{n=1}^{q} (S_{mn} - \mu_s)^2)(\sum_{m=1}^{N_r} \sum_{n=1}^{q} (\hat{S}^l_{mn} - \mu_{\hat{S}^l})^2)}}, \quad (20)$$

where S_{mn} and $\hat{S}^l_{mn}$ are the elements of matrices S and $\hat{S}^l$, respectively. Also, μ_s and $\mu_{\hat{S}^l}$ are the means of these matrices, respectively. Clearly, the set A_{l^*} with the maximum $\mid C_l \mid$ is selected to give the indices of N_r LEDs from which the ADR receives LOS signals. The index of selected set l^* can be obtained by:

$$\hat{S}^{l^*} = arg \max_{\hat{S}^l} \mid C_l \mid, \quad \forall l \in \{1, 2, \ldots, L\}. \quad (21)$$

The selected set of LEDs indices A_{l^*} is then used in channel estimation to determine the channel gains associated with these LEDs.

C. CHANNEL ESTIMATION

Two common methods are extensively used for channel estimation which are Least Square Error (LS) and Minimum Mean Square Error (MMSE) methods. Generally, MMSE achieves better performance but it requires good prior information about the channel. Also, it depends on the channel covariance matrix and the noise variance. Thus, suitable schemes must be found to estimate these parameters, or even assuming that estimates are available [15], [27], [35]. In the proposed IM-CFOV-CE scheme, the LS method is used for its simplicity; while MMSE can be used in future work.

Least square Error (LS): Here, the scheme aims to find the optimal values of channel coefficients that minimize the square error [27]. In the proposed scheme, the sum of square error for channel estimation is given by:

$$\varepsilon(H) = \|S - H\hat{S}^{l^*}\|^2 = (S - H\hat{S}^{l^*})^T (S - H\hat{S}^{l^*}), \quad (22)$$

The optimization criterion can be defined as:

$$\hat{H}_{LS} = arg \min_H \varepsilon(H), \quad (23)$$

By differentiating and setting derivative to zero i.e.,

$$\frac{\partial}{\partial H}(S - H\hat{S}^{l^*})^T (S - H\hat{S}^{l^*}) = 0, \quad (24)$$

The estimated channel gain matrix is then given by:

$$\hat{H}_{LS} = ((\hat{S}^{l^*})^T \hat{S}^{l^*})^{-1} (\hat{S}^{l^*})^T S, \quad (25)$$

Example 3: From the simulation of VLC downlink channel, indicated in Fig. 2, the estimated channel gain matrix at position (2.5, 2.5, 0.8), $\psi_{opt} = 31°$ and azimuth angle 0° is given by:

$$\hat{H}_{LS} = 1.0e-05 * \begin{bmatrix} 0.0007 & 0.0006 & 0.2316 & 0.2309 \\ 0.2308 & 0.0008 & 0.2317 & 0.0005 \\ 0.2315 & 0.2311 & 0.0006 & 0.0004 \\ 0.0006 & 0.2311 & 0.0006 & 0.2312 \end{bmatrix}. \quad (26)$$

Comparing the estimated channel gain matrix to the exact one given in (17), small errors less 0.1 percent occur in some estimated LOS gains and the proposed scheme efficiently estimates all the channel gains. After estimating the LOS channel gain $\hat{H}_{LS}$, it is exploited to resolve the interfered signals using Maximum-Likelihood (ML) detection.

D. MAXIMUM LIKELIHOOD DETECTION

Upon getting the channel gains associated with the interfered signal, proper channel equalization is carried to decode these signals. Among many exiting equalization techniques, Maximum Likelihood (ML) and Zero-Forcing equalizers (ZF) are the most common ones [36], [37]. However, ZF equalizer amplifies system noise by multiplying it with the inverse of the channel gain matrix. The amplification occurs for systems with small channel gain values and this represents a major drawback of ZF equalizer. As indicated in (17), the considered system has channel gains with small values and ZF equalizer is not recommended in this case. Therefore, maximum likelihood equalizer is used to decode the interfered signals in the proposed IM-CFOV-CE scheme. Although ML detection implies optimal detection, it requires complex calculations.

In ML detection, each possible combination of transmitted signal vector X is multiplied by the estimated channel gain matrix $\hat{H}_{LS}$ and the result is compared to the received signal vector Y. Then, the scheme chooses the transmitted signal $\hat{X}_{ML}$ that achieves the least Euclidean distance between received and the recovered transmitted signal as [37], [38]:

$$\hat{X}_{ML} = arg \min_X \|Y - \hat{H}_{LS}X\|^2. \quad (27)$$

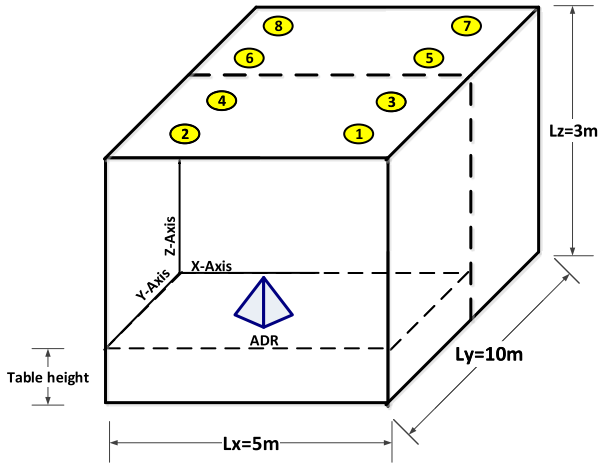

FIGURE 5. Room architecture.

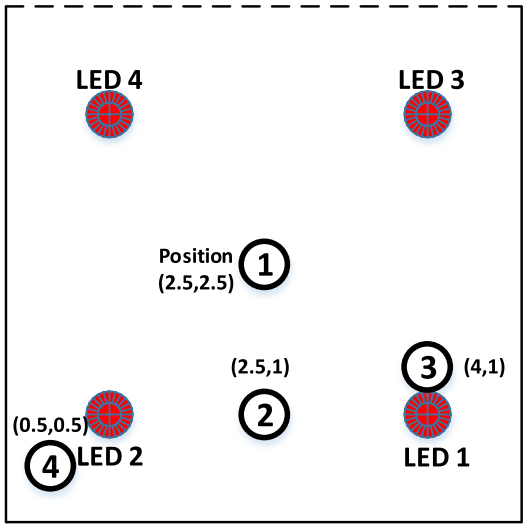

FIGURE 6. Different evaluation positions.

IV. PERFORMANCE EVALUATION

The optimization problem of constrained field of view ADR scheme is solved, and the optimum field of view angle ψ_{opt} is obtained for existing LED distribution. Then, the performance of the proposed IM-CFOV-CE scheme is compared with that of CFOV-ADR without CCI management scheme in terms of BER. The comparison is carried at different ADRs' positions, rotation angles, and heights. Clearly, for CFOV-ADR without CCI management, the detected signal on each PD is the one with highest received SINR while the other signals are considered as interfered signals. The SINR in this case is calculated from (28) as shown at the bottom of this page [39], where D^j is the desired LED for which the SINR at PD_i is calculated. Obviously, all received NLOS signals are considered as interfered signals as they arrive with different delays from decoded LOS signals.

A. SIMULATION PARAMETERS

The simulated room dimensions are $5m \times 10m \times 3m$ with eight LED transmitters ($N_t = 8$) installed at the ceiling ($z = 3m$). Only half of room is considered in the simulations due to the existing symmetry as indicated in Fig. 5. All LEDs are pointing straight down with elevation of 180°, and they transmit the same average optical power of P_T. A CFOV-ADR receiver with $N_r = 4$ PDs is used to receive data signals from all transmitted LEDs located within ADR's FOV. Let the ADR height be denoted by z_r, the Azimuth angle by γ_r and the elevation angle of all PDs by δ^i_{PD}. Additional simulation parameters are given in Table 1. The performance of the proposed IM-CFOV-CE scheme is investigated at four different positions as indicated in Fig. 6. These positions are the room center, the center between two LEDs, below a LED and at room corner.

TABLE 1. Simulation parameters.

Room parameters	Values
Room dimensions (L_x, L_y, L_z)	$5m \times 10m \times 3m$
Table height (z_r)	$0.8m$, $1.2m$
Wall reflection coefficient (ρ_k)	0.8
Reflective area of wall (ΔA)	$1\ cm^2$
Transmitters parameters	**Values**
Number of LEDs N_t	4
LEDs coordinates (x_t, y_t)	$(4,1), (1,1), (4,4), (1,4)$
LEDs elevation angle	180^o
LEDs azimuth angle	0^o
Semi half angle $\Phi_{1/2}$	45^o
Sampling period (T_s)	$0.5ns$
ADR receiver parameters	**Values**
Area of PD A	$1\ cm^2$
Number of PDs N_r	4
PDs Responsivity R	$1A/W$
PDs optimal FOV angle ψ_{opt}	31^o
Radius of receiver array (r)	$0.5cm$

B. OPTIMIZATION OF TILT ANGLE

Generally, the optimal FOV angle ψ_{opt} depends on aspects and locations of LED bulbs along with the geometry of ADRs. This is because the values of channel gains depend on angles and distances between LEDs and ADRs as indicated in equation 2. One of the main parameters of the ADR's geometry that affect the overall system performance is the PDs' tilt angle δ_{tilt}. With each value of δ_{tilt} there is an optimal FOV angle that satisfies the condition of equation (14) and it is obtained using dedicated exhaustive search. However, among all values of $\delta_{tilt} \in [0, \pi/2]$ there is an optimal tilt angle that gives the highest performance in terms of the average BER.

$$SINR_i(x_r, y_r, z_r, \gamma_r) = \frac{(Rh^{los}_{iD^i}(x_r, y_r, z_r, \gamma_r))^2}{\sigma^2_{n,i} + \sum_{j \neq D^i}^{N_t} (Rh^{los}_{ij}(x_r, y_r, z_r, \gamma_r))^2) + \sum_{j=1}^{N_t} (Rh^{Nlos}_{ij}(x_r, y_r, z_r, \gamma_r))^2)} \quad (28)$$

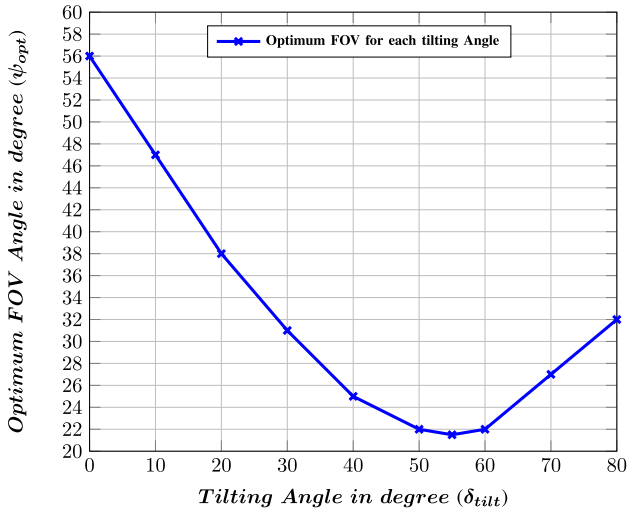

FIGURE 7. Optimum FOV angle versus ADR's tilt angle.

1) OPTIMUM FOV ANGLE

Figure 7 shows the optimal FOV angle ψ_{opt} for each tilt angle δ_{tilt}. The largest FOV angle is required at $\delta_{tilt} = 0°$ (horizontal PDs) because; the ADR at position 2 has to collect LOS signals from LEDs 1 and 2. By increasing the tilt angle from 0° to 55°, the PDs become more directed toward the LEDs resulting in lower optimum FOV angles. However, increasing the tilt angle over 55° requires increasing the FOV angles again to maintain the reception of LOS signals from the two LEDs.

2) BER PERFORMANCE

Figure 8 indicates the BER performance of the proposed IM-CFOV-ADR scheme versus receiver's azimuth angle γ_r at different positions, heights and tilt angles. The simulated tilt angles are 30°, 45° and 60°. At the four positions and for all values of the azimuth angle, the lowest BER occurs with $\delta_{tilt} = 30°$. However, for $\delta_{tilt} = 45°$ and 60°, Receiving LOS signals occurs at some azimuth angles. This is frequently observed with $\delta_{tilt} = 60°$ because its associated optimal FOV angle is narrow and equal to 22°. Obviously, the optimal tilt angle that gives the highest performance in terms of the average BER is near 30°. Therefore, the considered tilt angle in the rest of the simulations is $\delta_{tilt} = 30°$ with associated $\psi_{opt} = 31°$.

C. NUMBER OF DOWNLINK VLC CHANNELS

The proposed receiver design ensures downlink connectivity from different LEDs at most positions and orientations of the receiver. This enables smoother handover and full user mobility. Obviously, as the user moves away from the connected LEDs, it becomes closer to other LEDs at which the connections could be switched. Fig. 9 indicates the number of received LOS signals at each position in the room for receiver height of 0.8m, rotation angle of 0°, and tilt angle of 30°. Obviously, the proposed IM-CFOV-CE scheme enables receiving of more than one LOS signal over most

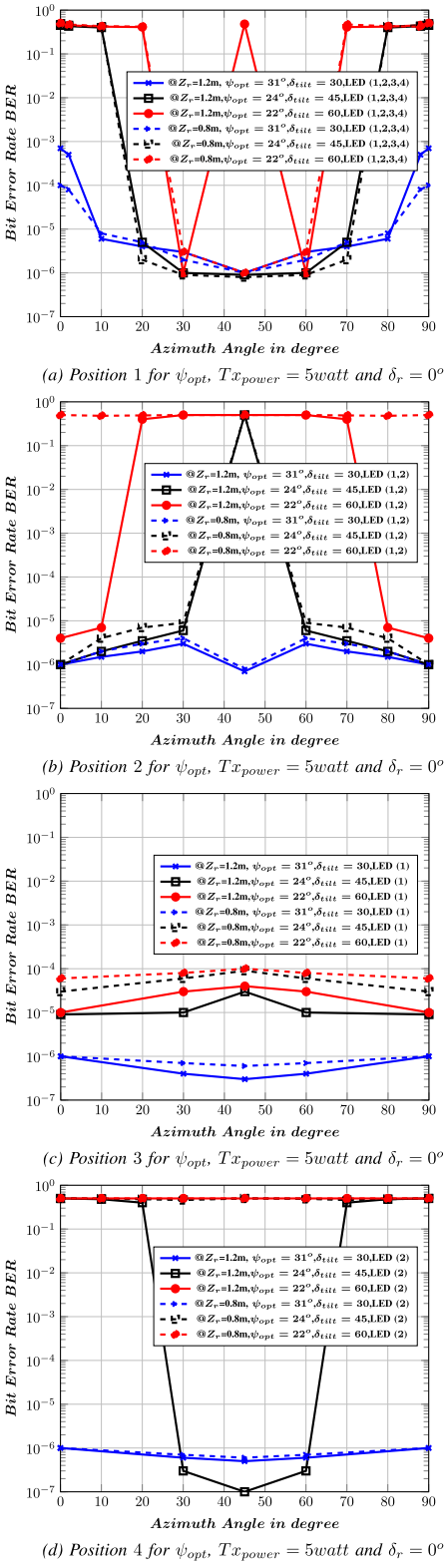

(a) Position 1 for ψ_{opt}, $Tx_{power} = 5watt$ and $\delta_r = 0^o$

(b) Position 2 for ψ_{opt}, $Tx_{power} = 5watt$ and $\delta_r = 0^o$

(c) Position 3 for ψ_{opt}, $Tx_{power} = 5watt$ and $\delta_r = 0^o$

(d) Position 4 for ψ_{opt}, $Tx_{power} = 5watt$ and $\delta_r = 0^o$

FIGURE 8. BER performance for different positions at different tilt angles.

positions. The green area represents the location where the proposed scheme can resolve four downlink VLC channels (signals). The red areas indicate the location where the scheme can resolve three signals. Moreover, the blue color

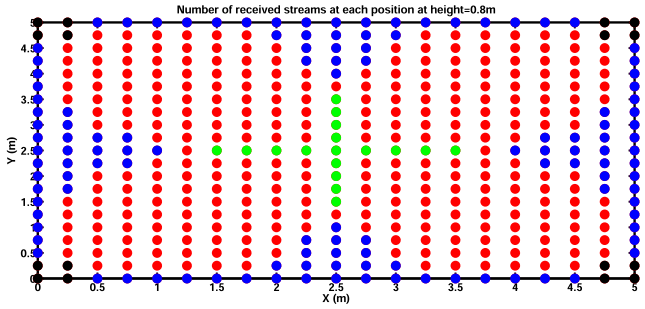

FIGURE 9. Number of resolved LOS signals using IM-CFOV-CE scheme through the room at $\psi_{opt} = 31°$, $\gamma_r = 0°$, $\delta_{tilt} = 30°$ and $z_r = 0.8m$. Green, red, blue and black colors indicate four, three, two and one receiving signals, respectively.

shows the areas of receiving two downlink channels, while the areas with one downlink channel represented by the black color. Clearly, the proposed scheme can provide multiple downlink channels for each user at most of the room positions resulting in significant enhancement of downlink capacity per user.

D. BER PERFORMANCE

The BER performance of the proposed IM-CFOV-CE scheme is investigated at four different positions as indicated in Fig. 6. The evaluations of BER performance at optimum tilting angle $\delta_{tilt} = 30°$ with optimum FOV $\psi_{opt} = 31°$ are considered against average transmitted power and rotation angle γ_r at various receiver heights z_r in the following subsections.

1) BER PERFORMANCE VERSUS AVERAGE TRANSMITTED POWER

Fig. 10 indicates the BER performance of the proposed IM-CFOV-CE scheme versus the average transmitted power at different room positions and receiver heights. The performance is compared with that of CFOV-ADR without CCI management. Generally, at all room positions the CFOV-ADR without CCI management performs worth than the proposed IM-CFOV-CE scheme in terms of achieved BER. As indicated in Fig. 10 (a), it can be noticed that at room center along with $\gamma_r = 0°$, the CFOV-ADR's PDs are approximately at the same distances and directions from the four transmitted LEDs 1, 2, 3, and 4 which results in severe CCI. For CFOV-ADR without CCI management, the BER is high and approximately the same for the two heights. This is because the interfered signals and the main signal have equal channel gains. In other words; CFOV-ADR has low SINR at this position. However, the BER performance of IM-CFOV-CE scheme is better, and these four interfered signals are detected with the same BERs. Additionally, at position 2 with $\gamma_r = 0°$ as shown in Figure 10 (b), the BER is the same for the two schemes. This is because one of the four PDs receives one LOS signal from LED 1 and another PD receives one LOS signal from LED 2. The other two PDs do not receive any LOS signals as their FOVs

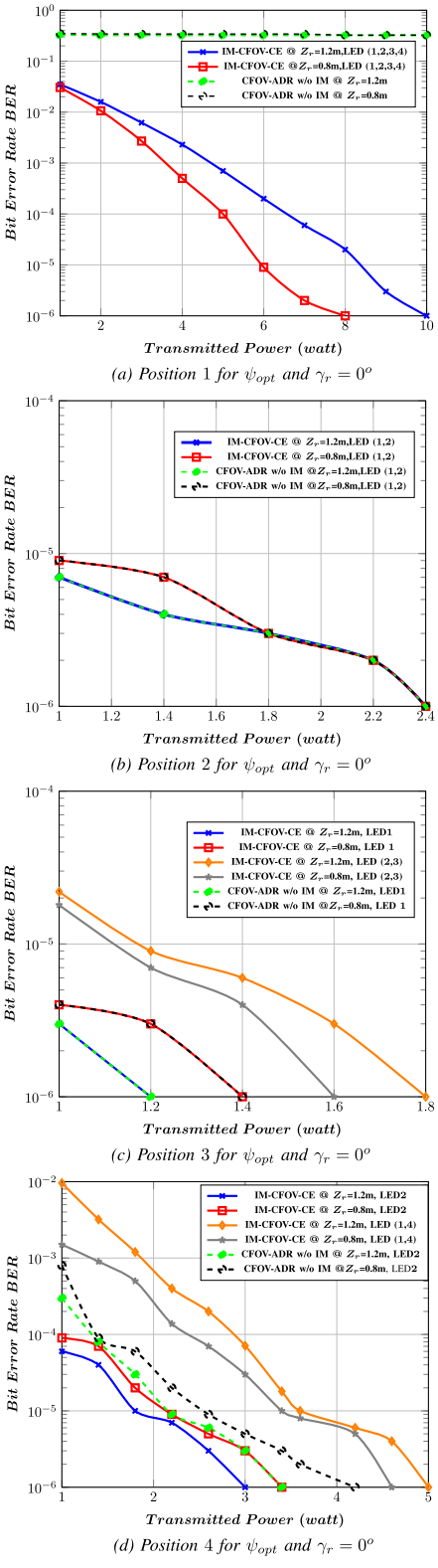

(a) Position 1 for ψ_{opt} and $\gamma_r = 0^o$

(b) Position 2 for ψ_{opt} and $\gamma_r = 0^o$

(c) Position 3 for ψ_{opt} and $\gamma_r = 0^o$

(d) Position 4 for ψ_{opt} and $\gamma_r = 0^o$

FIGURE 10. BER performance at different receiver positions and heights.

are constrained with condition of (14). In other words, no co-channel interference occurs at this position and orientation. Hence, both actual and estimated channel gains have a

slight difference resulting in near the same performance for both schemes. Moreover, at low transmitted powers, rising up the receiver increases the amount of received power resulting in less BER. However, at high transmitted power, increasing the receiver height has a negligible effect on the obtained BER because the received power becomes much larger than the system noise. For positions 3, and 4 with $\gamma_r = 0°$ as shown in Fig. 10 (c, d), the BER associated with nearest LED is lower than the BERs of other received LEDs. However, using proposed IM-CFOV-CE scheme, the BERs of other received LEDs decrease significantly by increasing the amount of transmitted power. Also, at position 3 the BER associated with LED 1 is the same for the two schemes because the ADR lies under the LED and high SINR is received at this position. However, using IM-CFOV-CE scheme, the interfered signals from LEDs 2 and 3 could be effectively detected. At position 4, the proposed IM-CFOV-CE scheme achieves lower BER for LED 2 than that of CFOV-ADR without IM due to the generated interferences from LEDs 1 and 4. Additionally, it's noticed that for position 2, 3, 4 by increasing the receiver height, the BER of the nearest LED decreased while the BERs of other LEDs increased. Clearly, decreasing receiver height will decrease the distance between the ADR and nearest LED which in turn increases the channel gain according to (2). Furthermore, increasing the receiver height will decrease the viewing angles between the ADR and far LEDs which in turn decreases their channel gains. However, for position 1 (center of the room), all LEDs have equal distances to the ADR and the channel gains are decreased by increasing the receiver height. This occurs because the decreasing of viewing angles between the ADR and all LEDs. Clearly, using proposed IM-CFOV-CE scheme, the number of received downlink channels could be significantly increased at most of room positions. Precisely, at positions 3 and 4, the proposed scheme enables the receiving from three different LEDs while the CFOV-ADR without IM can decode only one LOS signal. Moreover, IM-CFOV-CE scheme helps in increasing VLC downlink channel capacity with acceptable BER at position 1 where the most CCI occurs.

2) BER PERFORMANCE VERSUS ADR ROTATION

Here, the BER is calculated for the mentioned positions at different orientation angles γ_r from zero to 90° as the performance is repeated every 90°. Moreover, a performance symmetry exists around $\gamma_r = 45°$. Fig. 11 shows BER performance versus rotation angle γ_r at different heights z_r and fixed transmitted power $Tx_{power} = 5\ watt$ and fixed tilting angle $\delta_{tilt} = 30°$. For position 1 at receiver height of 1.2 m as indicated in Fig. 11 (a), the lowest and highest BER values are 10^{-6} and 10^{-4} which occur at $\gamma_r = 45°$ and $\gamma_r = 0°$, respectively. Clearly, at $\gamma_r = 45°$, each PD receives only one LOS signal without CCI resulting in the lowest BER value and maximum number of established downlink channels. Also, at this rotation angle both IM-CFOV-CE and CFOV-ADR without IM schemes achieve the same performance. Moreover, for $\gamma_r = 4°$ to 10°, the BER

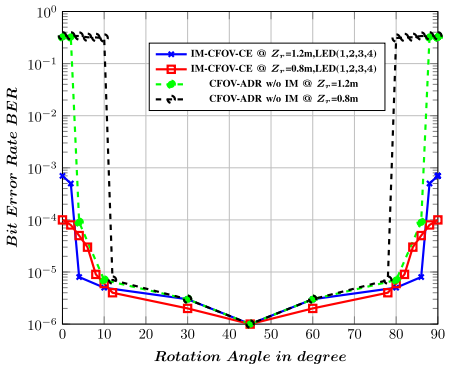

(a) Position 1 for ψ_{opt} and Tx_{power}=5watt

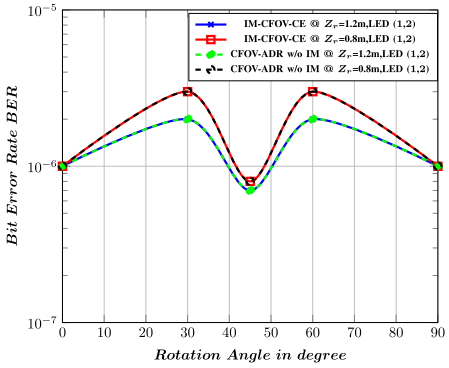

(b) Position 2 for ψ_{opt} and Tx_{power}=5watt

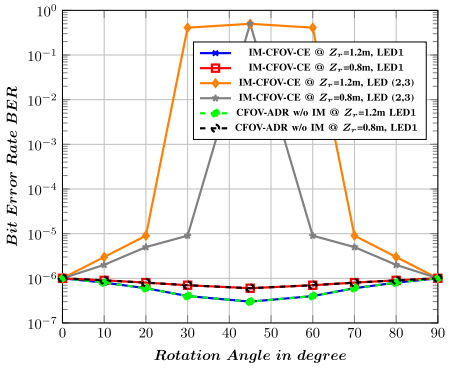

(c) Position 3 for ψ_{opt} and Tx_{power}=5watt

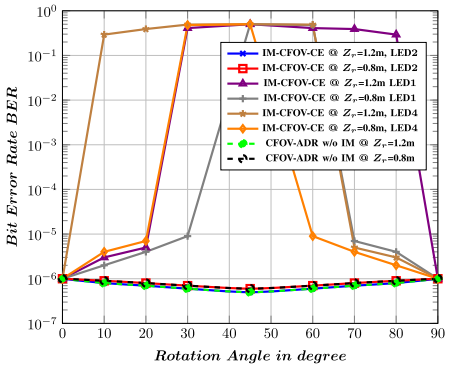

(d) Position 4 for ψ_{opt} and Tx_{power}=5watt

FIGURE 11. BER performance for different positions at different rotation angles.

of IM-CFOV-CE scheme decreases by increasing the receiver height due to deceasing FOV angles for interfered signals.

However, out of this range, the interfered signals become out of ADR's FOV and increasing receiver height decreases the LOS channel gains and consequently increases BER.

Generally, the PDs' FOV is optimized so that the ADR doesn't receive from more than N_r LEDs at any rotation angles. Hence, as shown in Fig. 11 (b) for position 2 and at any rotation angle, the BER is same for the two schemes because at this position the ADR receives LOS signals from LEDs 1 and 2 only without CCI. Also, it is worth noting that the BER is increased from $\gamma_r = 0°$ to $\gamma_r = 30°$, because the channel gains decrease. Then the BER is decreased from $\gamma_r = 30°$ to $\gamma_r = 45°$, and the BER reach its minimum (maximum channel gains) at $\gamma_r = 45°$. Moreover, increasing receiver height leads to increase the channel gains and decrease the BER.

Additionally, at positions 3 and 4 as shown in Figs. 11 (c and d), the BER of the nearest LED is the same for the two schemes and it decreases by increasing rotation angle γ_r from 0° to 45°. In contrast, using proposed IM-CFOV-CE scheme, the ADR can resolve the interfered LOS signals from other two LEDs with low BERs specially at rotation angles less than 30°. Also, at these positions, increasing ADR height increases the channel gains for the nearest LEDs while decreasing the gains for far ones.

In summary, the proposed IM-CFOV-CE scheme enable efficient decoding of interfered LOS signals at most positions and orientations of the ADR which significantly increases the downlink capacity for each user and facilities the handover and user mobility in VLC systems.

E. COMPARISON WITH TIME DIVISION MULTIPLE ACCESS (TDMA)

Time division multiple access TDMA and frequency division multiple access FDMA are the most common channelization techniques that could be used to solve CCI problems. Generally, FDMA is realized in downlink VLC channel by assigning different wavelengths to adjacent LED transmitters and then use optical filter at the receiver side to separate the received wavelengths. While in TDMA, different operating time slots are assigned to adjacent LEDs to avoid the CCI. In this subsection, a performance comparison between the proposed IM-CFOV-ADR scheme and TDMA is performed and a similar one could be carried for FDMA case.

Generally, to keep a constant illumination level in the room, each LED has to transmit the same average optical power in the two schemes. This means that in TDMA scheme and during each operating slot, one LED transmits data while its adjacent LEDs transmit DC light. In the case of IM-CFOV-ADR system, all LEDs are sending data simultaneously, and the transmitted power is used for both data and illumination.

However, to fairly compare the performance, in terms of the BER, of the proposed IM-CFOV-ADR scheme to that of TDMA scheme at position 1 in the simulated system, the received data rates have to be the same for both schemes. Clearly, at this position the IM-CFOV-ADR scheme can resolve the interference of four different data streams from

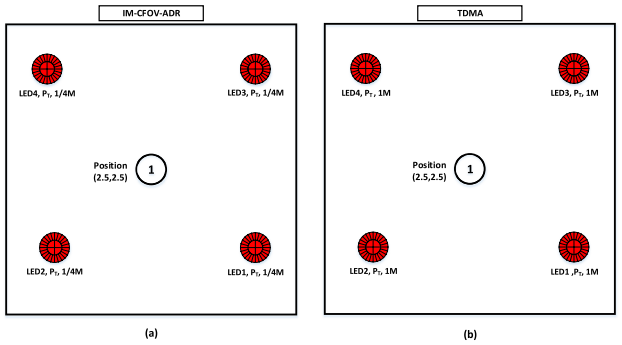

FIGURE 12. Comparison between IM-CFOV-ADR and TDMA schemes.

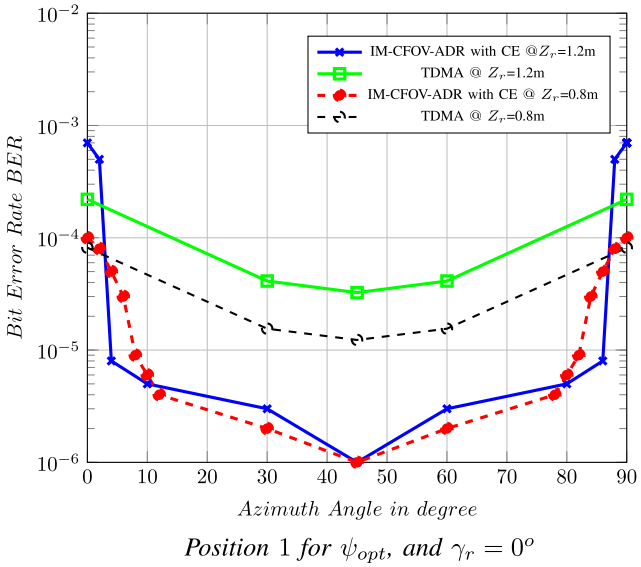

FIGURE 13. BER Comparison between IM-CFOV-ADR and TDMA at position 1.

four transmitters. Hence, each transmitter in IM-CFOV-ADR scheme is assumed to operate with quarter the transmission rate of TDMA case as indicated in Fig. 12. Clearly, this will increase the bit duration in IM-CFOV-ADR scheme. Consequently, for a fix transmitted power, the energy per bit in IM-CFOV-ADR scheme is higher than that in FDMA scheme resulting in lower BERs. Moreover, the same CFOV-ADRs that have PDs with the same FOV angle values are used in evaluating the two schemes. The OOK modulation is considered in the carried comparison with BER given in terms of SNR by [40]

$$BER_{OOK} = \frac{1}{2} erfc\left(\frac{1}{2}\sqrt{SNR}\right) \tag{28}$$

For a user located at position 1, Fig.13 indicates the BER performance of the two schemes versus the receiver's azimuth angle at two different receiver heights. Clearly, for small rotation angles less than 4 degrees, the TDMA achieves lower BERs levels than that of the proposed IM-CFOV-ADR scheme. This occurs because at these small rotation angles the proposed scheme faces high CCI levels.

However, increasing the receiver rotation angle decreases the CCI which in turn improves the performance of IM-CFOV-ADR scheme. In contrast, increasing the azimuth angle for TDMA scheme reduces the SNR of different PDs resulting in higher BERs. Moreover, the BER performance gap is increased by increasing azimuth angle and its maximum value occurs at $\gamma_r = 45°$ with a value of one order of magnitude. In summary, at most receiver positions and rotation angles, the BER performance and the number of received channels for IM-CFOV-ADR are better than that of TDMA schemes. In addition, the IM-CFOV-ADR scheme exploits the entire available optical and time spectrum to significant increase the downlink capacity over that of the traditional TDMA scheme.

V. CONCLUSION

The paper aims to increase number of VLC downlink channels for each user and to mitigate CCI resulting from implementing frequency reuse of one. The goals are achieved by designing an ADR with a limited field-of-view angle to reduce number of interfered LOS signals. Then, least-square channel estimation along with maximum-likelihood detection are used to resolve the interfered signals. The proposed scheme could effectively exploit co-channel interference from neighbor LEDs to increase downlink channel capacity. In addition, the proposed scheme is applicable for any LEDs layouts, provides flexibility, and facilitates the handover between LEDs. Simulation results reveal the superior performance of the proposed scheme over the one without interference management in terms of downlink capacity and BER at most receiver positions and orientations. The performance gap is maximized at room center where maximum CCI occurs. Also the proposed scheme is compared with TDMA and achieve higher performance than it at most receiver positions and rotation angles.

REFERENCES

[1] Cisco Visual Networking Index. (2016). *Global Mobile Data Traffic Forecast Update, 2015–2020 White Paper*. [Online]. Available: http://goo.gl/ylTuVx

[2] S. Singh, G. Kakamanshadi, and S. Gupta, "Visible light communication—An emerging wireless communication technology," in *Proc. 2nd Int. Conf. Recent Adv. Eng. Comput. Sci. (RAECS)*, Dec. 2015, pp. 1–3.

[3] L. Zeng, D. O'Brien, H. Minh, G. Faulkner, K. Lee, D. Jung, Y. Oh, and E. Won, "High data rate multiple input multiple output (MIMO) optical wireless communications using white led lighting," *IEEE J. Sel. Areas Commun.*, vol. 27, no. 9, pp. 1654–1662, Dec. 2009.

[4] T. Fath and H. Haas, "Performance comparison of MIMO techniques for optical wireless communications in indoor environments," *IEEE Trans. Commun.*, vol. 61, no. 2, pp. 733–742, Feb. 2013.

[5] T. Q. Wang, Y. A. Sekercioglu, and J. Armstrong, "Analysis of an optical wireless receiver using a hemispherical lens with application in MIMO visible light communications," *J. Lightw. Technol.*, vol. 31, no. 11, pp. 1744–1754, Jun. 1, 2013.

[6] T. Chen, L. Liu, B. Tu, Z. Zheng, and W. Hu, "High-spatial-diversity imaging receiver using fisheye lens for indoor MIMO VLCs," *IEEE Photon. Technol. Lett.*, vol. 26, no. 22, pp. 2260–2263, Nov. 15, 2014.

[7] K. D. Dambul, D. C. O'Brien, and G. Faulkner, "Indoor optical wireless MIMO system with an imaging receiver," *IEEE Photon. Technol. Lett.*, vol. 23, no. 2, pp. 97–99, Jan. 15, 2011.

[8] K.-H. Park and M.-S. Alouini, "Optimization of an angle-aided mirror diversity receiver for indoor MIMO-VLC systems," in *Proc. IEEE Global Commun. Conf. (GLOBECOM)*, Dec. 2016, pp. 1–6.

[9] A. Nuwanpriya, S.-W. Ho, and C. S. Chen, "Indoor MIMO visible light communications: Novel angle diversity receivers for mobile users," *IEEE J. Sel. Areas Commun.*, vol. 33, no. 9, pp. 1780–1792, Sep. 2015.

[10] P. Fahamuel, J. Thompson, and H. Haas, "Improved indoor VLC MIMO channel capacity using mobile receiver with angular diversity detectors," in *Proc. IEEE Global Commun. Conf.*, Dec. 2014, pp. 2060–2065.

[11] P. F. Mmbaga, J. Thompson, and H. Haas, "Performance analysis of indoor diffuse VLC MIMO channels using angular diversity detectors," *J. Lightw. Technol.*, vol. 34, no. 4, pp. 1254–1266, Feb. 15, 2016.

[12] A. Burton, Z. Ghassemlooy, S. Rajbhandari, and S.-K. Liaw, "Design and analysis of an angular-segmented full-mobility visible light communications receiver," *Trans. Emerg. Telecommun. Technol.*, vol. 25, no. 6, pp. 591–599, Jun. 2014.

[13] Z. Chen, N. Serafimovski, and H. Haas, "Angle diversity for an indoor cellular visible light communication system," in *Proc. IEEE 79th Veh. Technol. Conf. (VTC Spring)*, May 2014, pp. 1–5.

[14] A. Nuwanpriya, S.-W. Ho, and C. S. Chen, "Angle diversity receiver for indoor MIMO visible light communications," in *Proc. IEEE Globecom Workshops (GC Wkshps)*, Dec. 2014, pp. 444–449.

[15] Y. S. Hussein, M. Y. Alias, and A. A. Abdulkafi, "On performance analysis of LS and MMSE for channel estimation in VLC systems," in *Proc. IEEE 12th Int. Colloq. Signal Process. Appl. (CSPA)*, Mar. 2016, pp. 204–209.

[16] K. Ying, H. Qian, R. J. Baxley, and S. Yao, "Joint optimization of precoder and equalizer in MIMO VLC systems," *IEEE J. Sel. Areas Commun.*, vol. 33, no. 9, pp. 1949–1958, Sep. 2015.

[17] T. Fath, J. Klaue, and H. Haas, "Coded spatial modulation applied to optical wireless communications in indoor environments," in *Proc. WCNC*, Apr. 2012, pp. 1000–1004.

[18] O. Sayli, H. Dogan, and E. Panayirci, "On channel estimation in DC biased optical OFDM systems over VLC channels," in *Proc. Int. Conf. Adv. Technol. Commun. (ATC)*, Oct. 2016, pp. 147–151.

[19] A. Anusree and R. K. Jeyachitra, "Performance analysis of a MIMO VLC (Visible light Communication) using different equalizers," in *Proc. Int. Conf. Wireless Commun., Signal Process. Netw. (WiSPNET)*, Mar. 2016, pp. 43–46.

[20] A. Zafar, A. Khalid, and H. M. Asif, "Equalization techniques for visible light communication system," in *Proc. Int. Conf. Elect. Comput. Technol. Appl. (ICECTA)*, Nov. 2017, pp. 1–5.

[21] J. R. Barry, J. M. Kahn, W. J. Krause, E. A. Lee, and D. G. Messerschmitt, "Simulation of multipath impulse response for indoor wireless optical channels," *IEEE J. Sel. Areas Commun.*, vol. 11, no. 3, pp. 367–379, Apr. 1993.

[22] Z. Ghassemlooy, W. Popoola, and S. Rajbhandari, *Optical Wireless Communications: System and Channel Modelling with MATLAB*. Boca Raton, FL, USA: CRC Press, 2019.

[23] T. Komine and M. Nakagawa, "Fundamental analysis for visible-light communication system using LED lights," *IEEE Trans. Consum. Electron.*, vol. 50, no. 1, pp. 100–107, Feb. 2004.

[24] W. Zhong and Z. Wang, *Performance Enhancement Techniques for Indoor VLC Systems*. Cambridge, U.K.: Cambridge Univ. Press, 2015.

[25] C. Chen, W.-D. Zhong, H. Yang, S. Zhang, and P. Du, "Reduction of SINR fluctuation in indoor multi-cell VLC systems using optimized angle diversity receiver," *J. Lightw. Technol.*, vol. 36, no. 17, pp. 3603–3610, Sep. 1, 2018.

[26] Z. Wang, C. Yu, W.-D. Zhong, and J. Chen, "Performance improvement by tilting receiver plane in M-QAM OFDM visible light communications," *Opt. Express*, vol. 19, no. 14, pp. 13418–13427, Jul. 2011.

[27] S. M. Kay, *Fundamentals of Statistical Signal Processing: Detection Theory*. Upper Saddle River, NJ, USA: Prentice-Hall, 1993.

[28] I. Abdalla, M. B. Rahaim, and T. D. C. Little, "Dynamic FOV visible light communications receiver for dense optical networks," *IET Commun.*, vol. 13, no. 7, pp. 822–830, Apr. 2019.

[29] Thorlab. *Thorlab Mechanical Aperture Iris*. [Online]. Available: https://www.thorlabs.com

[30] J. F. Algorri, V. Urruchi, N. Bennis, P. Morawiak, J. M. Sanchez-Pena, and J. M. Oton, "Integral imaging capture system with tunable field of view based on liquid crystal microlenses," *IEEE Photon. Technol. Lett.*, vol. 28, no. 17, pp. 1854–1857, Sep. 1, 2016.

[31] T. G. Constandinou, J. Georgiou, and C. Andreou, "An ultra-low-power micro-optoelectromechanical tilt sensor," in *Proc. IEEE Int. Symp. Circuits Syst.*, May 2008, pp. 3158–3161.

[32] Q. Wang, D. Giustiniano, and M. Zuniga, "In light and in darkness, in motion and in stillness: A reliable and adaptive receiver for the Internet of lights," *IEEE J. Sel. Areas Commun.*, vol. 36, no. 1, pp. 149–161, Jan. 2017.
[33] A. K. Smilde, H. A. L. Kiers, S. Bijlsma, C. M. Rubingh, and M. J. van Erk, "Matrix correlations for high-dimensional data: The modified RV-coefficient," *Bioinformatics*, vol. 25, no. 3, pp. 401–405, Feb. 2008.
[34] D. J. Rumsey, *U Can: Statistics for Dummies*. Hoboken, NJ, USA: Wiley, 2015.
[35] H. Arslan and G. E. Bottomley, "Channel estimation in narrowband wireless communication systems," *Wireless Commun. Mobile Comput.*, vol. 1, no. 2, pp. 201–219, Apr. 2001.
[36] J. Ketonen, "Equalization and channel estimation algorithms and implementations for cellular MIMO-OFDM downlink," Ph.D. dissertation, Univ. Oulu, Oulu, Finland, 2012.
[37] R. Gupta and A. Grover, "BER performance analysis of MIMO systems using equalization techniques," *Innov. Syst. Des. Eng.*, vol. 3, no. 10, pp. 11–25, 2012.
[38] K. Su, "Efficient maximum likelihood detection for communication over multiple input multiple output channels," Dept. Eng., Univ. Cambridge, Cambridge, U.K., 2005.
[39] H. B. Eldeeb, H. A. I. Selmy, H. M. Elsayed, and R. I. Badr, "Interference mitigation and capacity enhancement using constraint field of view ADR in downlink VLC channel," *IET Commun.*, vol. 12, no. 16, pp. 1968–1978, Oct. 2018.
[40] T. Y. Elganimi, "Performance comparison between OOK, PPM and pam modulation schemes for free space optical (FSO) communication systems: Analytical study," *Int. J. Comput. Appl.*, vol. 79, no. 11, pp. 22–27, 2013.

MONA HOSNEY received the B.Sc. degree (Hons.) in communication and electrical engineering from Alexandria University. She is currently pursuing the M.Sc. degree with the Faculty of Engineering, Cairo University. She is also a Teacher Assistant with the National Telecommunication Institute (NTI), Cairo, Egypt. She is certified as an Optical Fiber Installation Instructor from Corning, Germany. She is also a Huawei HCIA Access Instructor. She joined the UNIX and Database Administration at Information Technology Institute (ITI), Cairo. She worked as a System Admin with Huawei Company. Her recent research interests include indoor visible light communication and optical fiber.

HOSSAM A. I. SELMY (Member, IEEE) was born in Giza, Egypt, in 1979. He received the B.S. and M.S. degrees from Cairo University, Cairo, Egypt, in 2001 and 2007, respectively, and the Ph.D. degree from Egypt–Japan University for Science and Technology (EJUST), Alexandria, Egypt, in 2013, all in electrical engineering. He is currently a Research Fellow with the Graduate School of Engineering, EJUST. He is also an Associate Professor with the National Institute of Laser Enhanced Science (NILES), Giza. His research interests include advanced modulations and multiple access schemes for optical fiber communications and next-generation wireless access networks.

ANAND SRIVASTAVA (Member, IEEE) received the M.Tech. and Ph.D. degrees from IIT Delhi. Before joining IIIT Delhi, he was the Dean and a Professor with the School of Computing and Electrical Engineering, IIT Mandi, India, and also an Adjunct Professor with IIT Delhi. Prior to this, he was with Alcatel-Lucent-Bell Labs, India, as a Solution Architect for access and core networks. Before joining Alcatel Lucent, he had a long stint (∼20 years) with the Center for Development of Telematics (CDOT), a telecom research center of Government of India, where he was the Director and a member of CDOT Board. During his stay in CDOT, he provided technical leadership and motivation to extremely qualified team of about more than 150 engineers engaged in the development of national level projects in the areas of telecom security systems, network management systems, intelligent networks, operations support systems, access networks (GPON), and optical technology-based products. Majority of these projects were completed successfully and commercially deployed in the public networks. He was also closely involved with ITU-T, Geneva in Study Group 15 and represented India for various optical networking standards meetings. His research interests include the area of optical core and access networks, vehicle to vehicle communications, fiber-wireless (FiWi) architectures, optical signal processing, free space optical communications, and energy aware optical networks.

KHALED M. F. ELSAYED (Senior Member, IEEE) received the B.Sc. degree (Hons.) in electrical engineering and the M.Sc. degree in engineering mathematics from Cairo University, Egypt, in 1987 and 1990, respectively, and the Ph.D. degree in computer science and computer engineering from North Carolina State University, in 1995. He is currently a Professor of communication networks and the Associate Department Head and the Coordinator of the Computing Group, Department of Electronics and Communications Engineering, Cairo University. His recent work focused on radio resource management and architectures for 4G/5G wireless systems, applications of machine learning in telecommunications, and devising scalable standards-based Internet of Things systems. He has more than 112 publications in international journals and conferences. He was a Member of Technical Staff at Nortel Networks, USA. He is also a Technical Fellow with Si-Vision working on low-power wireless systems using standards, such as Bluetooth low energy and thread as well as embedded machine learning architectures and algorithms. He has also been a member of the technical program committees and the Session Chair of several the IEEE, IFIP, and ITC conferences. He was the Chief Technical Officer with the Embedded Wireless Division in SySDSoft which was acquired by Intel, in March 2011. He was an Editor of the *IEEE Communications Magazine Internet Technology Series*, from November 1998 to December 2002.